SynOpen V. Lipson et al. THIEME OPEN ACCESS Paper

Low Molecular Weight Supramolecular Allobetuline-, Cyclohexanol-, or Undecanol-Appended 1,2,3-Triazole-Based Gelators: Synthesis and Molecular Dynamics Simulation Study

Victoria Lipson [a,b,c]*
Oleg Zhikol [a]
Svetlana Shishkina [a,b]
Alexander Semenenko [a]
Karina Kulyk [a]
Pavel Mateychenko [a]
Vladimir Musatov [a]
Alexander Mazepa [d]
Vladimir Vakula [a,c]
Alexander Borisov [e]
Alexander Kyrychenko [a,b]

[a] State Scientific Institution, 'Institute for Single Crystals' of the National Academy of Sciences of Ukraine, 60, Nauky ave., Kharkiv 61001, Ukraine
lipson@ukr.net
[b] School of Chemistry, V. N. Karazin Kharkiv National University, Kharkiv, Ukraine
[c] State Institution 'V. Ya. Danilevsky Institute for Endocrine Pathology Problems', National Academy of Medical Sciences of Ukraine, Kharkiv, Ukraine
[d] A. V. Bogatsky Physico-Chemical Institute of the National Academy of Sciences of Ukraine, Odessa, Ukraine
[e] ENAMINE Ltd, Kyiv, Ukraine

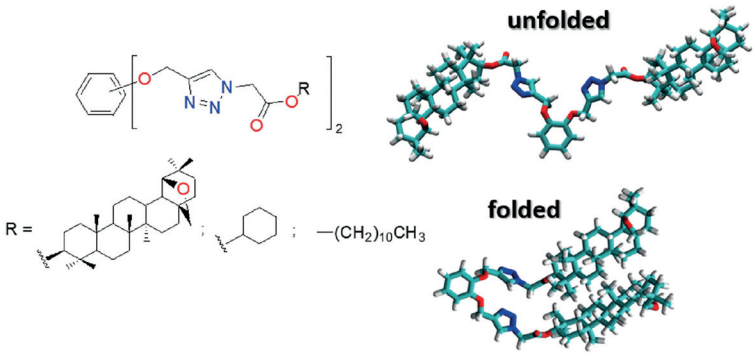

Received: 23.08.2023
Accepted after revision: 15.11.2023
Published online: 18.12.2023 (Version of Record)
DOI: 10.1055/s-0040-1720100; Art ID: SO-2023-08-0066-OP

Abstract Three novel isomeric supramolecular allobetuline-appended 1,2,3-triazole-based potential gelators and two model compounds with cyclohexanol or undecanol fragments in the structure instead of the triterpenoid platform were synthesized. Their ability to form gels in different solvents was studied experimentally and computationally by molecular dynamics simulations and quantum chemical calculations. We found that the gelling ability of such compounds is driven by the binding energy of intermolecular tail substituent interactions. The less significant factor is the molecule unfolding in a solvent, providing that the gelling substance is actually soluble. Preferred unfolded conformations were identified by classical molecular dynamics simulation and suggested the most prospective 1,2,3-triazole-based potential gelators.

Key words allobetuline, cyclohexanol, undecanol, supramolecular 1,2,3-triazole-based gelators, click reaction, molecular dynamics simulation, low-molecular-weight organogelator

Low-molecular-weight organogelators (LMWOGs) are currently an area of growing interest due to their physicochemical properties and potential practical applications in material science (photovoltaics, dye-sensitized solar cells), in resolving ecological problems (oil spill recovery), and medicine (wound healing, drug delivery).[1–6] One of the most challenging theoretical tasks in this field remains the prediction of the gelation ability of a targeted compound and understanding the mechanism of the self-assembly process in different solvents. Therefore, control of these processes would allow us to design materials with the desired properties.

Recently we have studied the synthesis and molecular modeling of three isomeric supramolecular dehydroepiandrosterone-appended 1,2,3-triazole-based gelators.[7] Continuing our research, here we report the synthesis and molecular modeling study of the three supramolecular allobetuline-, cyclohexanol-, or undecanol-appended 1,2,3-triazole-based potential gelators (TBGs, Figure 1). LMWOGs with triterpenoid or steroid scaffolds are attractive due to the presence in their structure of a hydrophobic molecular platform in the nanoscale range.[8–13] At the same time, the role of these fragments in gelation is still poorly understood. In this regard, we set ourselves the goal of finding out how the size and conformational mobility of the hydrophobic residue in molecules affect their ability for gelation.

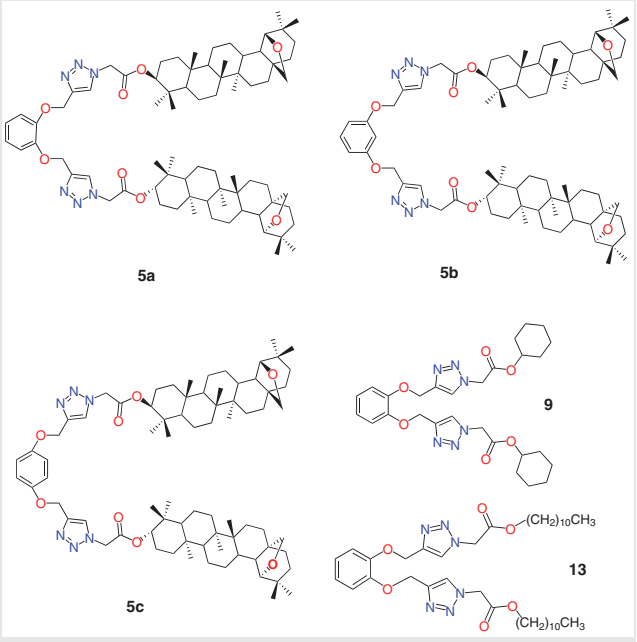

Figure 1 Molecular structures of the studied compounds

Synthesis

The compounds **5a–c**, **9**, and **13** were synthesized as shown in Scheme 1 by the synthetic procedures reported for dehydroepiadrosterone-based gelators in our previous study.[7] Briefly, the OH groups of allobetuline (**1**), cyclohexanol (**6**), and undecanol (**10**) were esterified with chloroacetyl chloride to compounds **2**, **7**, and **11**, respectively. The esters **2**, **7**, and **11** reacting with NaN_3 produced the azides **3**, **8**, and **12** with high yields. Cu(I)-catalyzed click reactions were pursued further on alkyne ethers **4a–c** using the azides **3**, **8**, and **12**. The target compounds **5a–c**, **9**, and **13** were fully characterized by routine spectroscopic methods.

Gelation Study

Gelation studies were carried out using the inversion tube method. The respective amounts (0.03 mmol) of compounds **5a–c**, **9**, and **13** were dissolved in 2 mL of the organic solvent, forming a homogeneous solution. The solution was heated and subsequently cooled to form a gel which generally was reluctant to flow upon tube inversion. The gelation properties of the synthesized compounds were examined in 12 solvents or mixtures of solvents (Table 1). Among all compounds and solvents studied, only allobetuline derivative **5a** in toluene has shown gelation (Figure 2).

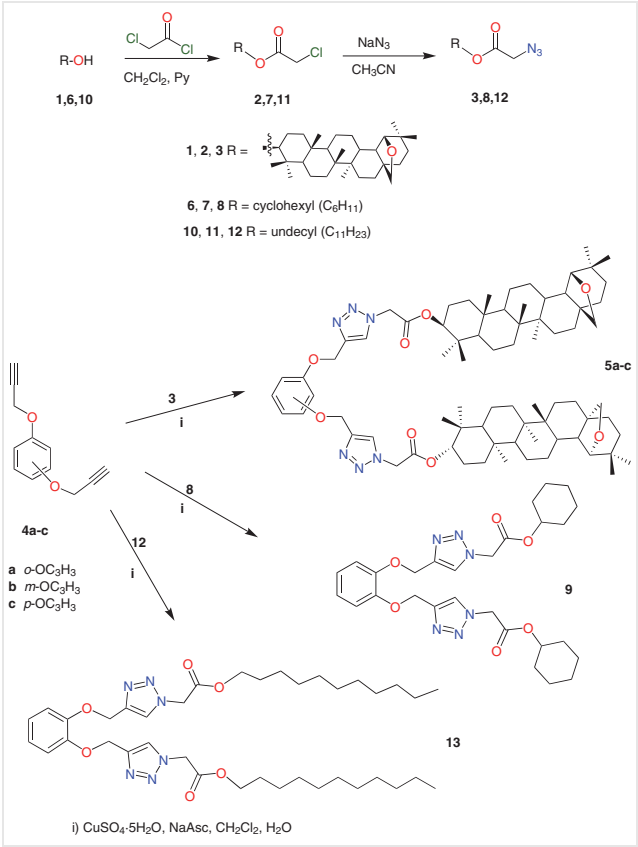

Scheme 1 Synthesis of the target compounds **5a–c**, **9**, and **13**

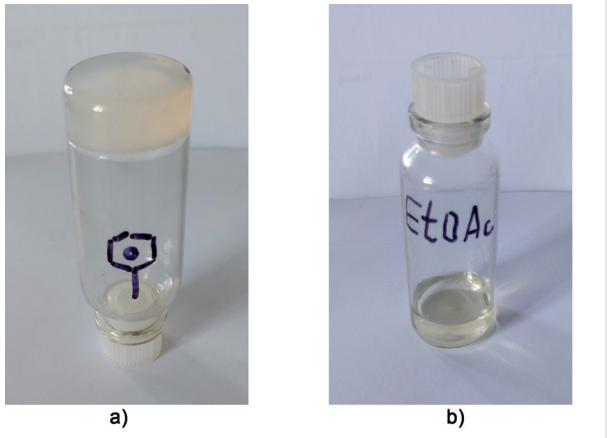

Figure 2 (a) Gel of compound **5a** in toluene; (b) solution of compound **5a** in EtOAc

The thermal stability of the gel, defined as the temperature T_g required for the organogel to collapse, was measured using the dropping ball method.[14,15]

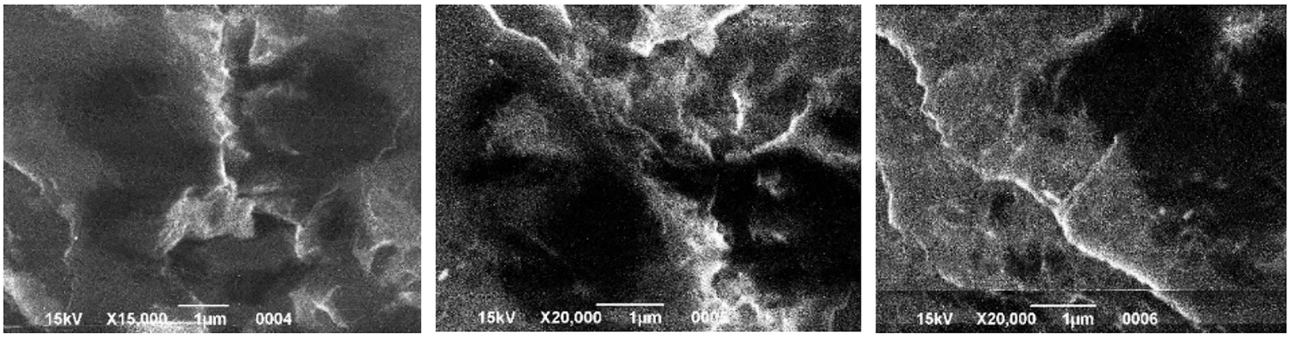

Figure 3 Scanning electron microscopy images of a dried gel of compound **5a**

Morphological Study of the Gel

Scanning electron microscopy (SEM) was used to get visual insights into the aggregation mode and the microscopic morphology of gel **5a**. SEM images were obtained by a JSM-6390LV instrument. SEM results show the microstructure of the xerogel obtained by drying gelator **5a** from toluene (Figure 3). The xerogel presents a solid uniform layer with surface defects like fissures, cavities, and other natural roughness, created at either stage of obtaining or preparation. The fibers seen at large magnifications cannot be regarded as a specific feature of the whole coating.

Molecular Dynamics Simulation Study

Taking into account the results of our previous study,[7] we evaluated the ability of allobetuline conjugates connected with aromatic spacer by 1,2,3-triazole linker to form gels in various organic solvents using MD simulations and DFT calculations. The obtained results were used to guide the synthesis of three isomeric compounds **5a–c**, followed by experimental probing of their gelling properties. The ability to form a gel was revealed only for conjugate **5a** in toluene (Table 1, Figure 2). Cyclohexanol **9** and undecanol **13** derivatives were obtained as model compounds that do not contain a developed molecular platform of the nanosize range; however, they have the same arrangement of substituents in the aromatic spacer as in the compound **5a**. These compounds did not form gels in any of the solvents tested (Table 1).

We consider an unfolded conformation of the solute molecule as a good prerequisite to form a stable 3D structure. The studied molecules are quite flexible, so that they may exhibit a small free energy difference between folded and unfolded conformations. The formed gels were highly temperature-sensitive, so they could be destroyed by a minimal heating. Therefore, even these small energy differences may be crucial. Unfolded molecules can interact via the tail (T) substituents. It is the preferred interaction mode for a gel formation. The parameters of the model considered here are following: (i) preferable conformations of a single TBG molecule in the solvent, and (ii) the intermolecular interaction energy of TBG molecules, bound mostly by tail substituents (TT interaction energy). This simplified model was utilized as some compromise instead of molecular dynamics (MD) simulates of a full gelation process: such a long-scale task would require considering several TBG molecules per a simulation cell and MD sampling for about 1000 ns long.[16–22]

The undecanol-appended TBG (compound **13**) differs from the other studied molecules by its essential conformational flexibility; therefore, it is examined in more detail. We found that the strongest binding interaction of two alkyl chains was observed in the case of parallel chain orientation. To maximize the interaction energy, these chains should also be maximally unfolded. In this conformation, the undecane C–C chain length reaches up to 1.25 nm. Our MD simulation gives average distance between the chain ends close to 1.05 nm, irrespectively from the *o*-, *m*-, *p*-sub-

Table 1 Gelling Capacity of Compounds **5a–c**, **9**, and **13** in Different Solvents[a]

	5a	5b	5c	9	13
MeOH	*I*	*I*	*I*	*S*	*P*
MeOH/CH_2Cl_2	*S*	*S*	*S*	*P*	*P*
toluene	*G*	*I*	*P*	*S*	*P*
CH_3CN	*I*	*I*	*I*	*S*	*P*
EtOAc	*S*	*I*	*P*	*S*	*S*
xylene	*P*	*I*	*P*	*P*	*P*
1,4-dioxane	*P*	*I*	*P*	*S*	*S*
cyclohexanol	*P*	*P*	*P*	*S*	*S*
EtOH	*I*	*I*	*I*	*P*	*P*
CH_2Cl_2	*S*	*S*	*S*	*S*	*S*
$CHCl_3$	*S*	*S*	*S*	*S*	*S*
DMSO	*P*	*P*	*P*	*S*	*S*

[a] *I* – insoluble, *S* – soluble, *C* – crystallization, *P* – precipitate, *G* – gel.

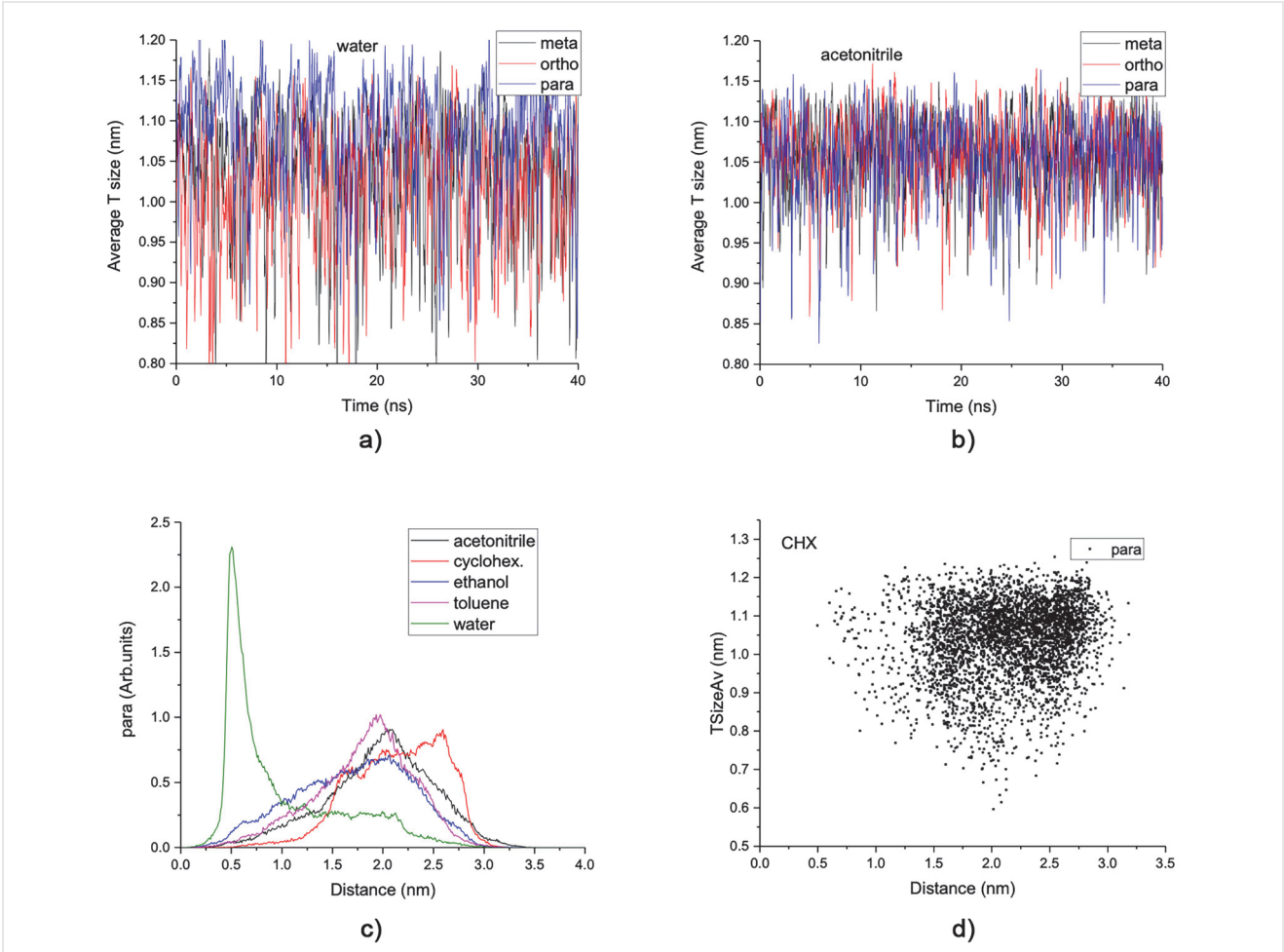

Figure 4 Time-traces of the size change of undecane tails in water (a) and acetonitrile (b). RDF plots of intramolecular TT distance for the *p*-isomer of undecanol-appended TBG in different solvents (c). A 2D plot of a TT distance versus tail size for the same isomer in cyclohexanol (d).

stitution type of the benzene ring, as well as from the solvent (Figures 4a and 4b). In a simple model of parallel chains, this adds 20% to the loss of TT interaction energy.

The dynamics of the fluctuation of varying tail substituent sizes during MD simulations had high amplitudes. The two limiting cases of the mean distance between the undecane chain tails, plotted as a running average over the MD trajectory, are presented in Figure 4 for water (a) and acetonitrile (b) solvents.

Visual comparison of the time-trace amplitudes for all five solvents reveals that the tail dynamics slow slightly in the following order: water > cyclohexanol > ethanol ≈ toluene > acetonitrile. We suggest the two factors, which could be operative here: solvent molecule size and solvent-solute interaction strength. In the presented sequence, the molecule size reduces (except water) and interaction strength increases. For water, we can have underestimated the solvent structuring, i.e., microscopic viscosity. Alkane chain vibrations are dominated by the internal chain elasticity and only modulated negligibly by the solvent. The dynamic fluctuations of undecane tail substituent size are too high, so the formation of stable solvate dimers through TT-interactions by undecanol-appended TBGs looks quite improbable.

We discuss further the conformational dynamics of the *o*-, *m*-, and *p*-isomers of TBGs with different tail substituents, such as undecanol, cyclohexanol, and allobetuline, by focusing on the substituent nature. We consider the distance between tail substituent C-atoms geometrical centers as the intramolecular TT distance used below.

Undecanol-appended TBGs. RDF plots for TT distance showed no preferred distance, which is indicative of a stable structure, for most studied solvents except for water (Figure 4c). The latter is due to the hydrophobic nature of the tail interaction in the water-undecane system. It causes the whole gelator molecule to adopt a folded conformation. The distribution maximum is systematically shifted to longer distances as the expected intramolecular TT increases for all following series of *o*-, *m*-, and *p*-substituted isomers. We can identify some slightly preferred solute conformation in cyclohexanol solvent due to the larger solvent mole-

cule size, i.e., due to the larger microscopic viscosity. The most promising results are found for the *p*-isomer in cyclohexanol (Figure 4d). In this system, the simultaneous unfolding of the undecane tails and the TBG molecule as a whole (Figure 4c) is the best, so, in this case, the gelation ability must be driven by the intermolecular TT interaction energy.

Cyclohexanol-appended TBGs. In this derivative, the tail substituent is smaller and much less conformationally flexible, compared to undecane discussed above. However, the nature of its interaction with solvents remains the same; the major contribution is due to hydrophobic or, more specifically, dispersion interactions.

Allobetuline-appended TBGs. In this derivative, the tail substituent is sufficiently large and contains an oxygen ether-type heteroatom. The heteroatom can form hydrogen bonding with protic solvents. However, it fills a small area of the molecular fragment surface and, unlike the carbonyl group in our previous study,[7] does not produce large dipole moment. Intermolecular TT interaction is still dominated by dispersion interactions.

Time-traces of intramolecular TT distances along 10 ns MD trajectory for *o*-, *m*-, and *p*-isomers in cyclohexanol are presented in Figure S4a (see the Supporting Information). Distance time-traces, averaged over eight molecules in the cell, are also presented in Figure S4b. Both graphs are similar enough irrespective of the model used and the timescale. It means that the effect is not affected by the extensive averaging. In this solvent, the TT distance dynamics are the slowest (probably, due to high microviscosity), while maintaining large enough TT distance. Another case of a slow TT distance dynamics is presented in water solution due to a collapse of TBG molecules down to a typical TT distance 0.8–1.2 nm. Table 2 summarizes the TT distance for the studied derivatives in different solvents.

Table 2 The Average TT Distance for Studied Derivatives (nm) in Different Solvents Estimated for One Molecule by MD Simulations

Solvent	5a	5b	5c	9	13
acetonitrile	2.0	2.4	2.6	2.2	1.3
cyclohexanol	2.4	2.9	3.2	2.4	1.4
Ethanol	2.5	3.0	3.1	2.0	1.2
Toluene	2.1	2.7	3.0	1.9	1.3
Water	0.8	2.4	2.9	0.8	0.7

In toluene, the distance dynamics is considerably higher, as seen in Figure 5a. On the other hand, only in this solvent, the preferred unfolded solvated conformation with a large TT distance around 2.5 nm was formed as seen in the corresponding RDF plots in Figure 5b and Table 2. Figure 5c demonstrates typical MD simulation snapshots for unfolded (*top*) and folded (*bottom*) conformations of derivatives **5a**–**c** in toluene.

Time-traces of intramolecular TT distances along the MD trajectory for *o*-, *m*-, and *p*-isomers in cyclohexanol reveal rather slow distance fluctuation. However, it is still characterized with high amplitude. It is displayed also by RDF plots of the same TT distance for the *o*-isomer (Supporting Information, Figure S5a) and *p*-isomer (Figure S5b) in different solvents. These two plots share the common features of solute molecule folding in water (the peaks around 0.7 nm) and unfolding in cyclohexanol (the peaks around 1.6–1.7 nm). Similarly, a larger solvent molecule elevates unfolded solute conformations. In the case of the *p*-isomer, the average TT distance is increased, however, at the same time, the specific fold for some conformations was lost and the RDF plots become smoother.

We can conclude that cyclohexanol is the solvent, which favors the gelation of the cyclohexane-appended TBG; however, the high TT distance dynamics impede the process. This factor might be overridden by large TT interaction energy, as discussed below.

Remarkably, the first RDF maximum of the *o*-isomer appears at the same 1.9 nm. In all other cases, the RDF plots are characterized with the unstructured pattern and the corresponding maxima for unfolded conformations are smoother and are found at a larger distance (the usual case of *p*-isomer).

The appearance of the unfolded conformation is one factor in our model. Another factor is the interaction energy of the tail substituents of different solute molecules. An example of a MD snapshot of the unfolded conformation of derivative **5a** stabilized by the intermolecular interactions of its allobetuline moieties is given in Figure S6 in the Supporting Information.

For precise energetic estimations of the stabilizing role of the tail-to-tail interactions, MP2 and DFT calculations were used. The quantum-chemical interaction energy for the set of the studied fragments is summarized in Table 3.

Table 3 Theoretically Estimated Interaction Energy (kcal/mol) of the TBG Tail Substituent Fragments

Fragment	Undecane	Cyclohexane	Allobetuline
interaction energy	−8.5[a]	−2.3[b], −2.8[c], −5.0[c]	−16.5[d]

[a] Roughly extrapolated from MP2 estimation for *n*-hexane.[20]
[b] Estimated by MP2.[21]
[c] Estimated by MP2 and wB97XD calculations.[22]
[d] Estimated by wB97XD (this work).

The interaction energy for the undecanol dimer represents definitely an upper limit, mainly due to very low probability of required ordering of the flexible alkyl chains in the liquid phase. Accounting just for 20% loss (estimated above from total chain length), we obtained ~7 kcal/mol,

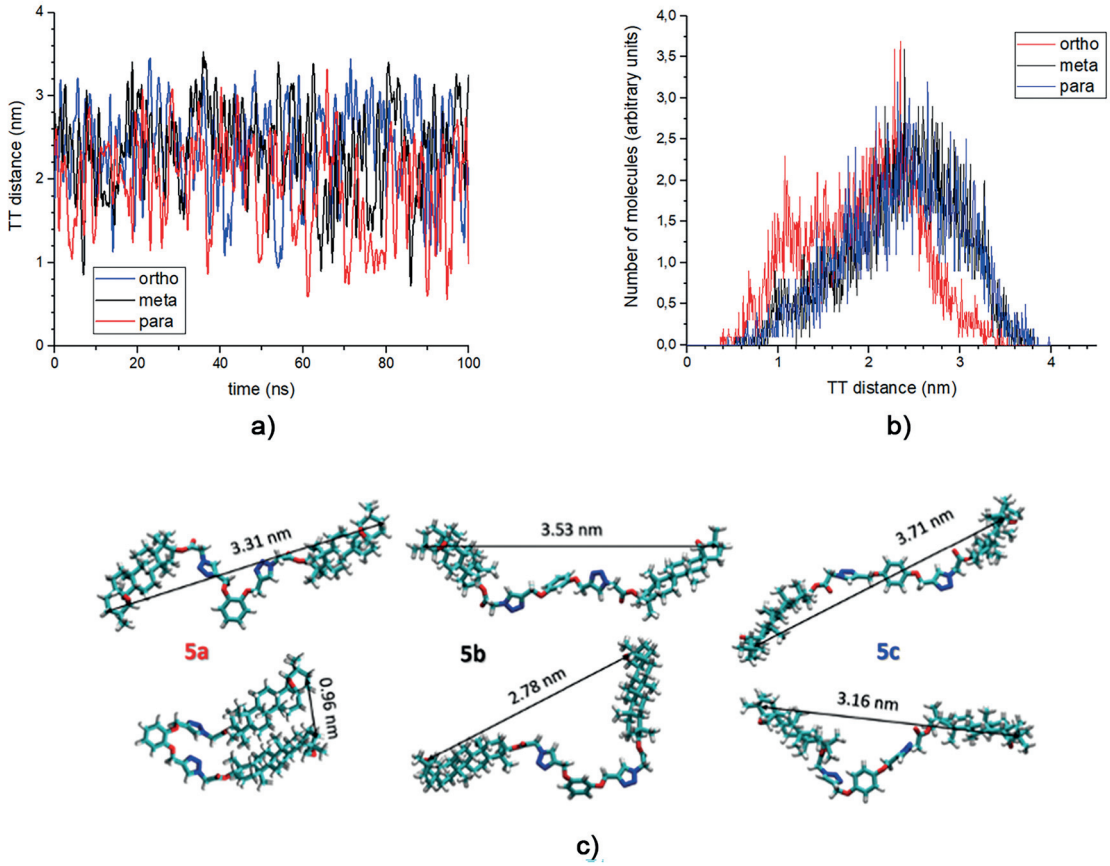

Figure 5 Intramolecular edge-to-edge distance dynamics for the three isomers **5a–c** of the allobetuline-appended TBG in toluene (a). RDF plots of the intramolecular edge-to-edge distance for the three isomers **5a–c** in toluene (b). Representative MD simulation snapshots for unfolded (*top*) and folded (*bottom*) conformations of **5a–c** in toluene. Arrows show the edge-to-edge distances.

and this number is still an upper limit. We would expect that the actual average energy is close to that for cyclohexane substituent, even despite the well-known underestimation the dispersion interaction energy by the MP2 method. On the other hand, the allobetuline dimer is characterized by about three times stronger interaction energy and compares well with the dehydroepiandrosterone dimer studied previously (the interaction energy estimated by the similar method was 11.5–14 kcal/mol).[7]

The discussed energies represent enthalpy or free energy at zero temperature. Accounting qualitatively for the finite temperature, we can note the following. While the allobetuline is the largest substituent, it prefers dispersion interactions in aprotic solvents. One fragment can interact either with several solvent molecules or with single similar fragment. In the latter case, the entropy loss will be smaller, so at higher temperatures the tail-tail interaction may become dominating over solvation.

The xerogel structure, shown in Figure 3, looks less ordered than in our previous study.[7] While the tail-tail interaction energy is similar for both allobetuline and dehydroepiandrosterone, the latter is characterized by more directed interaction in the dimer due to stacking-like arrangement of strongly dipolar carbonyl groups. It may be also the cause of the lesser ordering and lesser stability of allobetuline-appended TBGs compared to dehydroepiandrosterone appended ones.

Conclusions

1,2,3-Triazole-based molecules with benzene spacer and two tail substituents represent a prospective class of low-molecular-weight gelators. The gelling ability of such compounds is primarily driven by the energy of intermolecular tail substituent interactions. A less significant factor is the molecule unfolding in solvent, favoring the gelling substance becoming soluble. Nevertheless, preferred unfolded conformations found from classical MD simulation, allow us to suggest the most prospective TBGs. Finally, our computationally predicted structures were synthesized and tested for their gelling ability.

Materials and methods

All commercially available reagents and solvents were purchased from commercial vendors and used without purification. ^{1}H NMR and ^{13}C NMR spectra were recorded on a Varian MR-400 spectrometer 400 MHz and 100 MHz, respectively, in $CDCl_3$ without an internal reference. Elemental analyses were carried out on an EA 3000 Eurovector elemental analyzer. Melting points were determined on a Kofler hot bench. The progress of reactions and the purity of the obtained compounds were monitored by TLC on Alugrams Xtra SIL G/UV254 plates with CH_2Cl_2 as eluent. FAB-mass-spectrometric analyses were performed in the liquid matrix of *m*-nitrobenzyl alcohol using a magnetic sector mass spectrometer VG 70-70EQ equipped with a primary FAB ion source for generating a bombarding beam of argon atoms. The region of the molecular ion is represented by ion-radical M^+ and protonated molecular ion $[MH]^+$.

Allobetuline (**1**) was synthesized from commercially available betulin according to the procedure published previously.[23] Bis(prop-2-ynyloxy)benzenes **4a–c** were synthesized according to a well-known procedure.[8,24]

Allobetuline-3-chloroacetate (2)

Allobetuline (**1**; 10 g, 0.023 mol) was dissolved in CH_2Cl_2 (250 mL) with stirring; a catalytic amount of pyridine was added and chloroacetyl chloride (2.83 g, 0.025 mol) was added dropwise. The reaction was carried out under argon at r.t. monitored by TLC. Upon completion of the reaction, the solvent was removed under reduced pressure and the precipitate formed was crystallized (MeOH) to give **2** as a white amorphous powder; yield: 10.4 g (87%); mp 221–223 °C.

^{1}H NMR (400 MHz, $CDCl_3$): δ = 4.60–4.51 (m, 1 H, C^3H), 4.03 (s, 2 H, $COCH_2$), 3.75 (d, *J* = 7.8 Hz, 1 H, $C^{28}H^1$), 3.51 (s, 1 H, C^{19}H), 3.42 (d, *J* = 7.8 Hz, 1 H, $C^{28}H^2$), 0.96 (s, 3 H, CH_{3allo}), 0.91 (s, 3 H, CH_{3allo}), 0.89 (s, 3 H, CH_{3allo}), 0.86 (s, 6 H, 2 CH_{3allo}), 0.84 (s, 3 H, CH_{3allo}), 0.78 (s, 3 H, CH_{3allo}).

^{13}C NMR (126 MHz, $CDCl_3$): δ = 166.7 (CO), 87.5 (C^{19}), 85.8 (C^{28}), 82.9 (C^3), 70.8 (C^{17}), 55.1 (C^{18}), 50.5, 46.4, 41.0, 40.8, 40.3, 40.2, 38.1, 37.6 (2), 36.7, 36.3, 35.8, 33.7, 32.3, 28.3, 27.4, 26.0, 25.8, 24.1, 23.1, 20.6, 17.6, 16.1, 16.0, 15.2, 13.0.

MS (FAB): 519.2 (+FAB).

Anal. Calcd for $C_{32}H_{51}ClO_3$: C, 74.03; H, 9.90. Found: C, 74.07; H, 9.81.

Compounds **7** and **11** were synthesized by the same procedure.

Allobetuline-3-azidoacetate (3)

To a solution of chloroacetate **2** (5.2 g, 0.01 mol) in CH_3CN/dioxane (1:1, 200 mL) was added an excess of NaN_3 (1.3 g, 0.02 mol) and the mixture was boiled for 4 h until the reaction was complete (TLC monitoring). At the end of the process, CH_2Cl_2 was added to the cooled mixture, the inorganic precipitate was filtered off, and the excess solvent was removed under reduced pressure. The residue was crystallized (MeOH) to give **3** as an white amorphous powder; yield: 3.60 g (71%); mp 208–210 °C.

^{1}H NMR (400 MHz, $CDCl_3$): δ = 4.70–4.53 (m, 1 H, C^3H), 3.83 (s, 2 H, $COCH_2Cl$), 3.74 (d, *J* = 7.8 Hz, 1 H, $C^{28}H^1$), 3.50 (s, 1 H, C^{19}H), 3.41 (d, *J* = 7.8 Hz, 1 H, $C^{28}H^2$), 0.95 (s, 3 H, CH_{3allo}), 0.90 (s, 3 H, CH_{3allo}), 0.89 (s, 3 H, CH_{3allo}), 0.85 (s, 6 H, 2 CH_{3allo}), 0.84 (s, 3 H, CH_{3allo}), 0.77 (s, 3 H, CH_{3allo}).

^{13}C NMR (126 MHz, $CDCl_3$): δ = 168.1 (CO), 87.9 (C^{19}), 83.2 (C^{28}), 83.0(C^3), 71.2 (C^{17}), 55.5 (C^{18}), 51.0, 50.7, 46.8, 41.4, 40.7, 40.6, 38.5, 37.9, 37.1, 36.7, 36.2, 34.1, 33.8, 32.7, 28.8, 27.9, 26.4, 26.2, 24.5, 23.6, 21.0, 18.1, 16.5, 16.2, 15.7, 13.5.

MS (FAB): 525.7 (+FAB).

Anal. Calcd for $C_{32}H_{51}N_3O_3$: C, 73.10; H, 9.78; N, 7.99. Found: C, 73.01; H, 9.71; N, 7.53.

Compound **3** was used in the next step without further purification.

Compounds **8** and **12** were synthesized by the same procedure.

Benzene-1,2-bis((2-(4-methyloxy)-1*H*-1,2,3-triazol-1-yl)acetate-3-allobetuline) (5a)

Aq sodium ascorbate solution (0.10 g, 0.5 mmol) and aq $CuSO_4{\cdot}5H_2O$ solution (0.08 g, 0.32 mmol) were added to a stirred solution of azide **3** (1.00 g, 2.00 mmol) and **4a** (0.18 g, 0.97 mmol) in CH_2Cl_2 (20 mL) and left for 24 h under r.t. After completion of the reaction, the solvent was evaporated off under reduced pressure and the product was purified by column chromatography (CH_2Cl_2/EtOAc 9: 1) to give **5a** as a white powder; yield: 0.97 g (81%); mp 256–258 °C.

^{1}H NMR (400 MHz, $CDCl_3$): δ = 7.79 (s, 2 H, $CH_{triazole}$), 7.02 (s, 2 H, Ar), 6.91 (s, 2 H, Ar), 5.18 (d, 8 H, $4COCH_2$), 4.52 (d, 2 H, C^3H), 3.73 (d, *J* = 7.7 Hz, 2 H, $C^{28}H^1$), 3.49 (s, 2 H, C^{19}H), 3.41 (d, *J* = 7.7 Hz, 2 H, $C^{28}H^2$), 0.93 (s, 6 H, 2 CH_{3allo}), 0.89 (s, 6 H, 2 CH_{3allo}), 0.87 (s, 6 H, 2 CH_{3allo}), 0.82 (s, 6 H, 2 CH_{3allo}), 0.78 (s, 6 H, 2 CH_{3allo}), 0.76 (s, 6 H, 2 CH_{3allo}), 0.69 (s, 6 H, 2 CH_{3allo}).

^{13}C NMR (126 MHz, $CDCl_3$): δ = 165.5 (CO), 148.1 (2, Ar), 143.5, 121.8 (4, Ar), 115.1, 87.5, 83.3, 70.78, 55.0, 50.5, 46.4, 41.0, 40.3, 40.2, 38.0, 37.4, 36.7, 36.3, 35.8, 33.7, 33.3, 32.2, 28.3, 27.5, 25.9, 25.8, 24.1, 23.1, 20.6, 17.6, 16.0, 15.8, 15.2, 13.2.

MS (FAB): 1237.7 (+FAB).

Anal. Calcd for $C_{76}H_{112}N_6O_8$: C, 73.75; H, 9.12; N, 6.79. Found: C, 73.77; H, 9.08; N, 6.63.

Compounds **5b**,**c**, **9**, and **13** were synthesized by the same procedure.

Benzene-1,3-bis((2-(4-methyloxy)-1*H*-1,2,3-triazol-1-yl)acetate-3-allobetuline) (5b)

White powder; yield: 0.94 g (78%); mp 275–277 °C.

^{1}H NMR (400 MHz, $CDCl_3$): δ = 7.76 (s, 2 H, $CH_{triazole}$), 7.16 (s, 1 H, Ar), 6.59 (s, 3 H, Ar), 5.17 (d, 8 H, $4COCH_2$), 4.63–4.48 (m, 2 H, C^3H), 3.74 (s, 2 H, $C^{28}H^1$), 3.49 (s, 2 H, C^{19}H), 3.41 (d, *J* = 7.5 Hz, 2 H, $C^{28}H^2$), 0.94 (s, 6 H, 2 CH_{3allo}), 0.90 (s, 6 H, 2 CH_{3allo}), 0.88 (s, 6 H, 2 CH_{3allo}), 0.82 (s, 6 H, 2 CH_{3allo}), 0.78 (s, 6 H, 2 CH_{3allo}), 0.78 (s, 6 H, 2 CH_{3allo}), 0.70 (s, 6 H, 2 CH_{3allo}).

^{13}C NMR (126 MHz, $CDCl_3$): δ = 166.1 (CO), 158.9 (2, Ar), 142.6, 129.6 (Ar), 107.7 (3, Ar), 87.5, 83.5, 70.8, 55.0, 50.5, 46.4, 41.0, 40.3, 40.2, 38.0, 37.4, 36.7, 36.3, 35.8, 33.7, 33.3, 32.2, 28.3, 27.5, 26.0, 25.8, 24.1, 23.1, 20.6, 17.6, 16.0, 15.9, 15.2, 13.0.

MS (FAB): 1237.7 (+FAB).

Anal. Calcd for $C_{76}H_{112}N_6O_8$: C, 73.75; H, 9.12; N, 6.79. Found: C, 73.59; H, 9.06; N, 6.70.

Benzene-1,4-bis((2-(4-methyloxy)-1*H*-1,2,3-triazol-1-yl)acetate-3-allobetuline) (5c)

White powder; yield: 1.06 *g* (88%); mp 279–281 °C.

^{1}H NMR (400 MHz, $CDCl_3$): δ = 7.71 (s, 2 H, $CH_{triazole}$), 6.88 (s, 4 H, Ar), 5.14 (d, 8 H, $4COCH_2$), 4.62–4.47 (m, 2 H, C^3H), 3.74 (d, *J* = 7.8 Hz, 2 H, $C^{28}H^1$), 3.49 (s, 2 H, C^{19}H), 3.41 (d, *J* = 7.7 Hz, 2 H, $C^{28}H^2$), 0.94 (s, 6 H, 2 CH_{3allo}), 0.90 (s, 6 H, 2 CH_{3allo}), 0.88 (s, 6 H, 2 CH_{3allo}), 0.82 (s, 6 H, 2 CH_{3allo}), 0.79 (s, 6 H, 2 CH_{3allo}), 0.76 (s, 6 H, 2 CH_{3allo}), 0.71 (s, 6 H, 2 CH_{3allo}).

^{13}C NMR (126 MHz, $CDCl_3$): δ = 165.4 (CO), 152.3, 144.4, 142.9, 123.6, 115.4 (2, Ar), 87.5, 83.4, 70.8, 62.1, 55.0, 50.7, 50.5, 46.3, 41.0, 40.3, 40.2, 38.0, 37.4, 36.7, 36.3, 35.8, 33.7, 33.3, 32.2, 28.3, 27.5, 25.9, 25.8, 24.1, 23.1, 20.6, 17.6, 16.0, 15.9, 15.2, 13.0.

MS (FAB): 1237.7 (+FAB).

Anal. Calcd for $C_{76}H_{112}N_6O_8$: C, 73.75; H, 9.12; N, 6.79. Found: C, 73.62; H, 9.12; N, 6.68.

Cyclohexanol Chloroacetate (7)

Physicochemical characteristics of **7** correspond to those described in the literature.[25]

Yellow liquid; yield: 8.1 g (92%).

^{1}H NMR (400 MHz, $CDCl_3$): δ = 4.90–4.75 (m, 1 H, COOCH), 4.01 (s, 2 H, $COCH_2Cl$), 1.90–1.79 (m, 2 H, C^2H_2), 1.78–1.63 (m, 2 H, C^6H_2), 1.59–1.18 (m, 6 H, C_3H_6).

Anal. Calcd for $C_8H_{13}ClO_2$: C, 54.40; H, 7.42; Found: C, 53.97; H, 7.12.

Compound (**7**) was used in the next step without purification.

Cyclohexanol Azidoacetate (8)

Physicochemical characteristics of **8** correspond to those described in the literature.[26]

Yellow liquid; yield: 4.86 g (94%).

^{1}H NMR (400 MHz, $CDCl_3$): δ = 4.97–4.74 (m, 1 H, COOCH), 3.79 (s, 2 H, $COCH_2Cl$), 1.91–1.08 (m, 10 H, C_6H_{10}).

Anal. Calcd for $C_8H_{13}N_3O_2$: C, 52.45; H, 7.15; N, 22.94. Found: C, 52.27; H, 7.81; N, 22.67.

Compound **8** was used in the next step without purification.

Benzene-1,2-bis((2-(4-methyloxy)-1*H*-1,2,3-triazol-1-yl)acetate-cyclohexanol) (9)

White powder; yield: 0.60 g (78%); mp 120–122 °C.

^{1}H NMR (400 MHz, $CDCl_3$): δ = 7.74 (s, 2 H, $CH_{triazole}$), 7.05–6.96 (m, 2 H, Ar), 6.93–6.85 (m, 2 H, Ar), 5.20 (s, 4 H, $2COCH_2$), 5.07 (s, 4 H, $2CO-CH_2$), 4.85–4.74 (m, 2 H, COOCH), 1.83–1.73 (m, 4 H, $2C^2H_2$), 1.69–1.58 (m, 4 H, $2C^6H_2$), 1.53–1.14 (m, 12 H, $2C_3H_6$).

^{13}C NMR (126 MHz, $CDCl_3$): δ = 165.3(CO), 148.1 (2, Ar), 144.1, 124.2, 121.7 (2, Ar), 115.0, 74.7, 62.0, 50.6, 30.9, 26.7, 23.0.

MS (FAB): 553 (+FAB).

Anal. Calcd for $C_{28}H_{36}N_6O_6$: C, 60.86; H, 6.57; N, 15.21. Found: C, 60.68; H, 7.01; N, 14.96.

Undecanol Chloroacetate (11)

Physicochemical characteristics of **11** correspond to those described in the literature.[27]

Yellow liquid; yield: 6.58 g (91%).

^{1}H NMR (400 MHz, $CDCl_3$): δ = 4.16 (t, *J* = 6.7 Hz, 2 H, $COOCH_2$), 4.04 (s, 2 H, $COCH_2Cl$), 1.64 (p, *J* = 6.9 Hz, 2 H, $COOCH_2CH_2$), 1.39–1.16 (m, 16 H, C_9H_{16}), 0.86 (t, *J* = 6.7 Hz, 3 H, CH_3).

Anal. Calcd for $C_{13}H_{25}ClO_2$: C, 62.76; H, 10.13. Found: C, 62.37; H, 9.81.

Compound **11** was used in the next step without purification.

Undecanol Azidoacetate (12)

Yellow liquid; yield: 4.76 g (93%).

^{1}H NMR (400 MHz, $CDCl_3$): δ = 4.16 (t, *J* = 6.7 Hz, 2 H, $COOCH_2$), 3.84 (s, 2 H, $COCH_2N_3$), 1.64 (p, *J* = 6.9 Hz, 2 H, $COOCH_2CH_2$), 1.42–1.10 (m, 16 H, C_9H_{16}), 0.86 (t, *J* = 6.7 Hz, 3 H, CH_3).

^{13}C NMR (126 MHz, $CDCl_3$): δ = 168.3 (CO), 66.0(-OCH_2-), 50.3 (-CH_2-N_3), 31.8, 29.5, 29.5, 29.4, 29.3, 29.1, 28.5, 25.8, 22.6, 14.0 (CH_3).

Anal. Calcd for $C_{13}H_{25}N_3O_2$: C, 61.1; H, 9.7; N, 16.5. Found: C, 62.07; H, 10.01; N, 15.22.

Compound **12** was used in the next step without further purification.

Benzene-1,2-bis((2-(4-methyloxy)-1*H*-1,2,3-triazol-1-yl)acetate-undecanol) (13)

White powder; yield: 0.61 g (89%); mp 90–92 °C.

^{1}H NMR (400 MHz, $CDCl_3$): δ = 7.78 (s, 2 H, $CH_{triazole}$), 7.08–6.92 (m, 2 H, Ar), 6.97–6.86 (m, 2 H, Ar), 5.24 (s, 4 H, $2COCH_2$), 5.13 (s, 4 H, $2CO-CH_2$), 4.15 (t, *J* = 6.7 Hz, 4 H, $2COOCH_2$), 1.60 (d, *J* = 8.3 Hz, 4 H, $2COOCH_2CH_2$), 1.24 (s, 32 H, $2C_8H_{16}$), 0.86 (t, *J* = 6.6 Hz, 6 H, $2CH_3$).

^{13}C NMR (126 MHz, $CDCl_3$): δ = 165.9 (CO), 148.1 (Ar), 144.1(triazole), 124.5(triazole), 121.8 (Ar), 115.0, 66.0 (Ar-O-CH_2-), 63.0 (-CO-OCH_2-), 50.3 (N-CH_2-CO-), 31.4, 29.1, 29.1, 29.0, 28.8, 28.7, 27.9, 25.2, 22.2, 13.6 (CH_3).

MS (FAB): 697 (+FAB).

Anal. Calcd for $C_{38}H_{60}N_6O_6$: C, 65.49; H, 8.68; N, 12.06. Found: C, 65.22; H, 8.49; N, 11.84.

Determination of Gel-Sol Transition Temperature (T_g)

During measurements, a small glass ball was carefully placed on top of the studied gel, which was presented in a test tube. The tube was slowly heated in a thermostatic oil bath until the ball fell to the bottom of the test tube. The temperature at which the ball reaches the bottom of the test tube is taken as T_g of that system. T_g for gel obtained from compound **5a** in toluene is 40–42 °C.

Computational Chemistry Details

Classical molecular dynamics simulations were used to study the structure of all substitution isomers (*o*-, *m*-, *p*- in the benzene ring) of the synthesized compounds from Figure 1 in the five solvents: water, EtOH, cyclohexanol, CH_3CN, and toluene.

The all-atom OPLS/AA force field[28] was used as implemented in the GROMACS package.[29] FF preparation details are described in our previous work.[7] A single gelator molecule per cubic cell with 35–45 Å edge was used as a model for an ideal solution with solute concentration kept within 2–5% by weight. The simulation protocol for an ideal solution has the following steps: (1) a brief initial thermalization; (2) 40 ns of productive MD simulation at 298 K; (3) 40 ns of simulated annealing from 25 to 60 °C; (4) 40 ns of productive MD simulation at 333 K; (5) 40 ns of simulated cooling from 60 to 25 °C; and (6) 40 ns of productive MD simulation at 25 °C. The last MD trajectory was used for analysis. In addition, for the undecane-appended structure, two gelator molecules with close to dimeric arrangement per a simulation cell were also MD-sampled for 2–3 initial geometry guesses for 40 ns at 25 °C. Moreover, for the prospective allobetuline-appended structures, 80 ns of MD trajectories were generated for systems composed of 8 gelator molecules per a simulation cell.

The binding interaction energy of allobetuline substituents was estimated by DFT calculations with the wB97XD/cc-pvdz[30] level, which utilizes an empirical correction for dispersion interaction.

Analysis of the MD trajectories was carried out with the integrated GROMACS tools. Visualization was done using the VMD viewer.[31]

Conflict of Interest

The authors declare no conflict of interest.

Funding Information

The authors thank the National Academy of Sciences of Ukraine for financial support in the frame of the projects «Development of methodology «click»-chemistry for create components for advanced complexing materials» (0117U001280).

Acknowledgment

The authors thank all brave defenders of Ukraine who allow us to continue our scientific work and complete this research in besieged Kharkiv.

Supporting Information

Supporting information for this article is available online at https://doi.org/10.1055/s-0040-1720100.

References

(1) Pérez-Ruiz, R.; Díaz Díaz, D. *Soft Matter* **2015**, *11*, 5180.
(2) Lim, H. C.; Min, S. H.; Lee, E.; Jang, J.; Kim, S. H.; Hong, J.-I. *ACS Appl. Mater. Interfaces* **2015**, *7*, 11069.
(3) Steed, J. W. *Chem. Commun.* **2011**, *47*, 1379.
(4) Ibrahim, M. M.; Hafez, S. A.; Mahdy, M. M. *Asian J. Pharm. Sci.* **2013**, *8*, 48.
(5) Meng, Y.; Yang, Y. *Electrochem. Commun.* **2007**, *9*, 1428.
(6) Chen, S.; Tong, X. Q.; He, H. W.; Ma, M.; Shi, Y. Q.; Wang, X. *ACS Appl. Mater. Interfaces* **2017**, *9*, 11924.
(7) Zhikol, O. A.; Shishkina, S. V.; Lipson, V. V.; Semenenko, A. N.; Mazepa, A. V.; Borisov, A. V.; Mateychenko, P. V. *New J. Chem.* **2019**, *43*, 13112.
(8) Ghosh, K.; Panja, A.; Panja, S. *New J. Chem.* **2016**, *40*, 3476.
(9) Bag, B. G.; Dinda, S. K.; Dey, P. P.; Mallia, V. A.; Weiss, R. G. *Langmuir* **2009**, *25*, 8663.
(10) Ramírez-López, P.; de la Torre, M. C.; Asenjo, M.; Ramírez-Castellanos, J.; González-Calbet, J. M.; Rodríguez-Gimeno, A.; Ramírez de Arellano, C.; Sierra, M. A. *Chem. Commun.* **2011**, *47*, 10281.
(11) Gao, A.; Li, Y.; Lv, H.; Liu, D.; Zhao, N.; Ding, Q.; Cao, X. *New J. Chem.* **2017**, *41*, 7924.
(12) Lu, J.; Hu, J.; Song, Y.; Ju, Y. *Org. Lett.* **2011**, *13*, 2011.
(13) Panja, A.; Ghosh, S.; Ghosh, K. *New J. Chem.* **2019**, *43*, 10270.
(14) Takahashi, A.; Sakai, M.; Kato, T. *Polym. J.* **1980**, *12*, 335.
(15) Tan, H. M.; Moet, A.; Hiltner, A.; Baer, E. *Macromolecules* **1983**, *16*, 28.
(16) McCullagh, M.; Prytkova, T.; Tonzani, S.; Winter, N. D.; Schatz, G. C. *J. Phys. Chem. B* **2008**, *112*, 10388.
(17) Frederix, P. W. J. M.; Scott, G. G.; Abul-Haija, Y. M.; Kalafatovic, D.; Pappas, C. G.; Javid, N.; Hunt, N. T.; Ulijn, R. V.; Tuttle, T. *Nat. Chem.* **2015**, *7*, 30.
(18) Lee, O.-S.; Cho, V.; Schatz, G. C. *Nano Lett.* **2012**, *12*, 4907.
(19) Velichko, Y. S.; Stupp, S. I.; de la Cruz, M. O. *J. Phys. Chem. B* **2008**, *112*, 2326.
(20) Tsuzuki, S.; Honda, K.; Uchimaru, T.; Mikami, M. *J. Phys. Chem. A* **2004**, *108*, 10311.
(21) Jalkanen, J.-P.; Pakkanen, T. A.; Rowley, R. L. *J. Chem. Phys.* **2004**, *120*, 1705.
(22) Kim, K. S.; Karthikeyan, S.; Singh, N. J. *J. Chem. Theory Comput.* **2011**, *7*, 3471.
(23) Krasutsky, P. A.; Carlson, R. M.; Karim, R. US 2002128210, **2002**.
(24) Bi, J.; Zeng, X.; Tian, D.; Li, H. *Org. Lett.* **2016**, *18*, 1092.
(25) Bodor, N.; El-Koussi, A. A.; Kano, M.; Khalifa, M. M. *J. Med. Chem.* **1988**, *31*, 1651.
(26) Venuti, M. C.; Alvarez, R.; Bruno, J. J.; Strosberg, A. M.; Gu, L.; Chiang, H. S.; Massey, I. J.; Chu, N.; Fried, J. H. *J. Med. Chem.* **1988**, *31*, 2145.
(27) Dega-Szafran, Z.; Dulewicz, E.; Brycki, B. *ARKIVOC* **2007**, *(vi)*, 90.
(28) Kahn, K.; Bruice, T. C. *J. Comput. Chem.* **2002**, *23*, 977.
(29) Berendsen, H. J. C.; van der Spoel, D.; van Drunen, R. *Comput. Phys. Commun.* **1995**, *91*, 43.
(30) Frisch, M. J.; Trucks, G. W.; Schlegel, H. B.; Scuseria, G. E.; Robb, M. A.; Cheeseman, J. R.; Scalmani, G.; Barone, V.; Mennucci, B.; Petersson, G. A.; Nakatsuji, H.; Caricato, M.; Li, X.; Hratchian, H. P.; Izmaylov, A. F.; Bloino, J.; Zheng, G.; Sonnenberg, J. L.; Hada, M.; Ehara, M.; Toyota, K.; Fukuda, R.; Hasegawa, J.; Ishida, M.; Nakajima, T.; Honda, Y.; Kitao, O.; Nakai, H.; Vreven, T.; Montgomery, J. A.; Peralta, J. E.; Ogliaro, F.; Bearpark, M.; Heyd, J. J.; Brothers, E.; Kudin, K. N.; Staroverov, V. N.; Kobayashi, R.; Normand, J.; Raghavachari, K.; Rendell, A.; Burant, J. C.; Iyengar, S. S.; Tomasi, J.; Cossi, M.; Rega, N.; Millam, J. M.; Klene, M.; Knox, J. E.; Cross, J. B.; Bakken, V.; Adamo, C.; Jaramillo, J.; Gomperts, R.; Stratmann, R. E.; Yazyev, O.; Austin, A. J.; Cammi, R.; Pomelli, C.; Ochterski, J. W.; Martin, R. L.; Morokuma, K.; Zakrzewski, V. G.; Voth, G. A.; Salvador, P.; Dannenberg, J. J.; Dapprich, S.; Daniels, A. D.; Farkas, O.; Foresman, J. B.; Ortiz, J. V.; Cioslowski, J.; Fox, D. J. *Gaussian 09, Revision B01*; Gaussian, Inc: Wallingford CT, **2009**.
(31) Humphrey, W.; Dalke, A.; Schulten, K. *J. Mol. Graphics* **1996**, *14*, 33.